INSTITUTE OF PHYSICS PUBLISHING SEMICONDUCTOR SCIENCE AND TECHNOLOGY

Semicond. Sci. Technol. **21** (2006) 124–130 doi:10.1088/0268-1242/21/2/004

Current- and capacitance-voltage characteristics of Cd/p-GaTe Schottky barrier diodes under hydrostatic pressure

G Çankaya[1] **and B Abay**[2]

[1] Gaziosmanpaşa Üniversitesi, Fen-Edebiyat Fakültesi, Fizik Bölümü, Tokat, Turkey
[2] Atatürk Üniversitesi, Fen-Edebiyat Fakültesi, Fizik Bölümü, 25240 Erzurum, Turkey

E-mail: babay@atauni.edu.tr

Received 27 July 2005, in final form 23 November 2005
Published 21 December 2005
Online at stacks.iop.org/SST/21/124

Abstract

Schottky barrier diodes (SBDs) on p-type GaTe have been fabricated by Cd metallization and characterized by current–voltage (I–V) and capacitance–voltage (C–V) techniques as a function of hydrostatic pressure (0.0–7.0 kbar). The evaluation of the experimental data reveals a decrease of barrier height (Φ_b), ideality factor (n) and series resistance (R_s) with an increase in the hydrostatic pressure. The zero-bias barrier height, ideality factor and series resistance values for the Cd/p-GaTe SBD by I–V measurements have been in the range of 0.743–0.682 eV, 1.246–1.219 and 30.5–16.4 Ω for the 0.0–7.0 kbar pressure interval, respectively. C–V measurements at 1.0 MHz have resulted in higher barrier heights than those obtained from I–V measurements. The discrepancy between Schottky barrier heights (SBHs) obtained from I–V and C–V measurements is explained by the introduction of a spatial distribution of SBHs due to barrier height inhomogeneities that prevail in the metal/GaTe interface. The change of barrier height values ($\Phi_b(0) - \Phi_b(P)$) obtained from the I–V and C–V techniques turns out to have a mean linear pressure coefficient of -8.77 ± 0.10 meV kbar^{-1} ($= -87.7 \pm 1.0$ eV GPa^{-1}), approximately equal to that found for the band gap of GaTe. We have concluded that the variation of the barrier height due to the applied pressure should follow precisely the variation of the semiconductor band gap, accepting that the Fermi level is a reference level which is pinned to the conduction-band minimum (CBM) as a function of the pressure.

1. Introduction

Metal–semiconductor (MS) structures are important research tools for the characterization of new semiconductor materials, and the fabrication of these structures plays a crucial role in constructing some useful devices in technology. This highly productive characteristic of MS structures can be merged with the unique feature of layered crystals, which have covalently bonded two-dimensional sandwich layers that are separated from each other along the third dimension c by only weak interlayer interactions and are often referred to as van der Waals-like [1], to obtain some useful knowledge in this area of semiconductor technology.

III–VI compound semiconductors also have layered structures and can easily be cleaved across their van der Waals gap between the layers which leads to the outer surfaces closely resembling the inner ones. This cleavage planes have been found to be free of dangling bonds and proved to be inert to chemical reactions, and these features lead us to consider them as idealized substrates for the investigation of fundamental aspects of surface or interface reactions [2]. It has also been proposed that layered semiconductors may have a new application field with their potential use in decoupling the strain induced by lattice mismatch [3, 4].

Nevertheless, it is well known that the van der Waals planes contain non-idealities in the form of chalcogen

vacancies and steps [5]. Moreover, the crystal structures of III–VI semiconductors give rise to anisotropic features in the transport, optical and mechanical properties, and nonlinearity in the pressure and temperature dependence of some physical quantities.

Among III–VI layered crystals, GaTe is one of the less known semiconductors due to its complex crystal structure. It is a relatively new material with a direct band gap of 1.67 eV at room temperature and attracts researchers because of its application potential in optoelectronic device fabrication. Although structural, electrical, optical absorption and photoluminescence properties [6–19] have been widely investigated, there have been only a few studies on metal/GaTe Schottky barrier diodes (SBDs) [20–22].

It is well known that optical and electrical properties of semiconductors are sensitive to the application of external pressure and to the variations in temperature. Numerous studies using pressure as a research tool for the investigation of the semiconductor properties have been carried out, especially the hydrostatic pressure effects on the SBD characteristics in recent years [23–27].

There have been only a few reports on SBDs fabricated using III–VI layered semiconductors [18, 20–23, 28–31] and to the best of our knowledge none of them have given the pressure-dependent current–voltage and capacitance–voltage characteristics and barrier parameters of metal/p-GaTe SBDs. It would be interesting to research the hydrostatic pressure dependence of Cd/p-GaTe SBD parameters such as the ideality factor, barrier height and series resistance, and this paper presents our novel results on them by using I–V and C–V measurements.

2. Experimental details

Single crystals of GaTe were grown by a directional freezing method from a stoichiometric melt of 6 N gallium and 5 N tellurium starting materials, obtained from Alfa Aesar, in a carbon-coated and vacuum-sealed quartz ampoules with a tip at the bottom. Synthesis and the growth procedure were carried out in the same tube without breaking vacuum to minimize contamination. Details of the experimental procedure for the crystal growth were reported elsewhere [7]. Hall effect measurements indicated that the concentration of the holes is 1.6×10^{16} cm^{-3} at 300 K. The mobility attains a value of 60 cm^2 V^{-1} s^{-1} at 300 K and 900 cm^2 V^{-1} s^{-1} at 90 K, which were the best values among the reported ones [7]. The samples (with about 8×10 mm^2 area and 100–300 μm thickness) were cut from the freshly cleaved sheets with a razor blade (no further polishing or cleaning treatment was required because of the natural mirror-like cleavage faces of the samples) and inserted into the deposition chamber immediately. Ohmic contacts of low resistance on the backside of the samples were formed by evaporating indium followed by a heat treatment at 220 °C for 3 min in nitrogen atmosphere. The Schottky contacts were formed on the other faces by evaporating Cd as dots with a diameter of 1.0 mm. The evaporating process was carried out in a turbo molecular vacuum-coating unit at about 2×10^{-6} mbar. The device was placed on the specially designed probe station just after fabrication and inserted in a home-made piston-cylinder type pressure chamber given in detail in [25]. Special transformer oil was used as a pressure transmitting medium to ensure hydrostatic conditions. Ambient pressure was measured with the change in the resistance of the calibrated manganin wire. I–V characteristics of the devices were measured by a computer-controlled Keithley 487 picoammeter/voltage source and C–V characteristics by a HP4280A capacitance meter at 1 MHz modulation frequency. The hydrostatic pressure ranged from 0.0 to 7.0 kbar for both I–V and C–V measurements, and all the experiments were carried out at room temperature and in the dark.

3. Results and discussion

3.1. I–V measurements

The current (I) across an SBD at forward bias (V), based on the thermionic emission (TE) theory, is given by [32]

$$I = AA^*T^2 \exp\left(-\frac{q\Phi_b}{kT}\right)\left[\exp\left(\frac{qV}{nkT}\right) - 1\right], \qquad (1)$$

where A is the effective diode area, A^* is the effective Richardson constant, found to be 119.4 A K^{-2} cm^{-2} for the p-type GaTe from $A^* = 120m^*_{h\perp}$ where $m^*_{h\perp}(= 0.995m_0)$ is the effective mass of holes perpendicular to the layer plane [19, 33], T is the temperature, q is the electronic charge, k is the Boltzmann constant, Φ_b is the barrier height (BH), V is the voltage applied and n is the ideality factor.

The effect of the series resistance for an SBD is usually modelled with a series combination of a diode and a resistor R_s. The voltage V_d across the diode can be expressed in terms of the total voltage drop V across the diode and the resistor R_s. Thus, $V_d = V - IR_s$ and equation (1) can be expressed as

$$I = AA^*T^2 \exp\left(-\frac{q\Phi_b}{kT}\right)\left[\exp\left(\frac{q(V - IR_s)}{nkT}\right) - 1\right]. \qquad (2)$$

The saturation current is given by

$$I_0 = AA^*T^2 \exp\left(-\frac{q\Phi_b}{kT}\right) \qquad (3)$$

and is derived from the intercept of the straight line in the semi-logarithmic I–V plot for zero bias. Hence, the values for the BH Φ_b and the ideality factor n of an SBD can be extracted from the intercept and the slope of the linear portion of the semi-logarithmic I–V plot, respectively, while the R_s data are deduced from the best fit of experimental I–V data in equation (2). However, several different methods to extract the series resistance R_s of an SBD have been suggested. In our case, we have applied the methods proposed by Cheung [34]. Cheung's functions can be obtained from equation (2) as follows:

$$\frac{dV}{d(\ln I)} = IR_s + n\left(\frac{kT}{q}\right), \qquad (4)$$

$$H(I) = V - n\left(\frac{kT}{q}\right)\ln\left(\frac{I}{AA^*T^2}\right), \qquad (5)$$

where $H(I)$ can be written as

$$H(I) = IR_s + n\Phi_b, \qquad (6)$$

and where Φ_b is the BH obtained from the data of the downward curvature region in the forward bias I–V characteristic. Equation (4) should give a straight line for

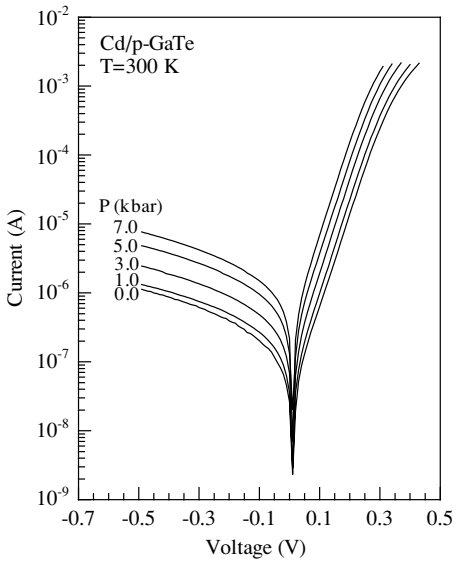

Figure 1. Current–voltage characteristics for the Cd/p-GaTe SBD as a function of hydrostatic pressure in the range of 0.0–7.0 kbar.

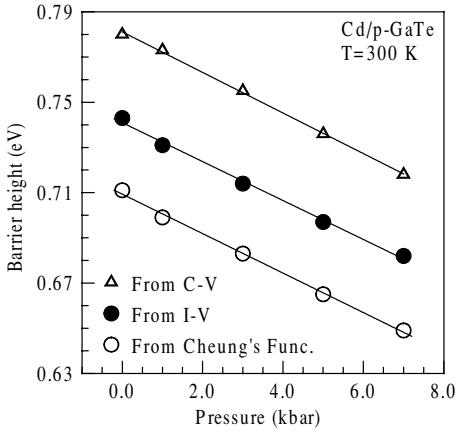

Figure 2. Pressure dependence of the BH determined by I–V and C–V characteristics for the Cd/p-GaTe SBD.

the data of downward curvature in the forward bias I–V characteristics. Thus, the slope and the y-axis intercept of the plot of $\mathrm{d}V/\mathrm{d}(\ln I)$ versus I will give R_s and nkT/q, respectively. Using the n value determined from equation (4) and the data of the downward curvature region in the forward bias region in equation (5), a plot of $H(I)$ versus I according to equation (6) will also give a straight line with the y-axis intercept equal to $n\Phi_b$. The slope of this plot also provides a second determination of R_s that can be used to check the consistency of Cheung's approach.

Figure 1 shows the semi-logarithmic forward and reverse bias I–V characteristics of a Cd/p-GaTe SBD in the pressure range of 0.0–7.0 kbar. These plots clearly depict the linearity between I and V over several orders of current. Furthermore, as shown in figure 1, the current flowing across the diode increases and the downward curvature portion in the forward bias region becomes progressively straight with increasing pressure. The variation of the BH, Φ_b, has been calculated from the y-axis intercepts of the semilog-forward bias I–V characteristics according to equation (3) as a function of pressure and is shown in figure 2 as filled circles. The BH values range from 0.743 eV at 0.0 kbar to 0.682 eV at 7.0 kbar (table 1). The decrease of Φ_b with the increase in the pressure is due to increasing of saturation current I_0 with increasing pressure.

The values of the ideality factor n are calculated from the slope of the linear portion of the forward bias I–V characteristics according to equation (2) for different pressures. As can be seen in table 1, the values of the ideality factor n obtained from figure 1 have decreased from 1.252 to 1.227 with increasing pressure. These values of the ideality factor are greater than unity. This can be due in part to defects induced by the cleaving process of the GaTe having van der Waals planes containing non-idealities in the form of chalcogen vacancies and steps, and/or the presence of a thin insulating layer, probably a native oxide layer, between the Cd and GaTe interface as the crystal is exposed to air just before the fabrication of the rectifier contact [5, 35]. In addition, Schottky barrier height (SBH) inhomogeneities, image-force effect, recombination-generation and tunnelling may be possible mechanisms leading to greater values for the ideality factor than unity [35–37].

For the alternative determination of Φ_b, n and R_s, the plots of Cheung's functions are given in figures 3 and 4 for measured data as a function of pressure. Least-squares fits have been used to evaluate the values of n and Φ_b for different pressures from the vertical axis intercepts of $\mathrm{d}V/\mathrm{d}(\ln I)$–$I$ and $H(I)$–I curves, and the values of R_s from their slopes, which are also given in table 1. As can be seen in table 1, the values of the ideality factor n, the BH Φ_b and the series resistance R_s obtained from figures 1, 3 and 4 have decreased with increasing pressure. Pressure dependence of the BH obtained from Cheung's functions is also plotted in figure 2 as open circles. The values of the R_s obtained from the best fit of the experimental I–V data in equation (2), $\mathrm{d}V/\mathrm{d}(\ln I)$–$I$ and $H(I)$–I plots are approximately equal to each other. This case shows the consistency of Cheung's approach and therefore, it is a common practice to take the averages of them. Figure 5 shows the plot of the averaged series resistance for the

Table 1. The experimentally obtained diode parameters for Cd/p-GaTe SBDs from I–V and C–V characteristics under hydrostatic pressure.

	I–V			$\mathrm{d}V/\mathrm{d}(\ln I)$–$I$		$H(I)$–I		C–V	
P (kbar)	n	Φ_b (eV)	R_s (Ω)	n	R_s (Ω)	Φ_b (eV)	R_s(Ω)	Φ_b (eV)	N_i (cm^{-3})
0.0	1.252	0.743	31.10	1.239	27.60	0.711	32.70	0.780	2.411×10^{16}
1.0	1.247	0.731	27.15	1.237	23.23	0.699	28.66	0.773	2.421×10^{16}
3.0	1.239	0.714	21.35	1.229	18.83	0.683	23.50	0.755	2.423×10^{16}
5.0	1.233	0.697	17.80	1.217	15.32	0.665	19.42	0.736	2.425×10^{16}
7.0	1.227	0.682	16.20	1.211	14.33	0.649	18.98	0.718	2.427×10^{16}

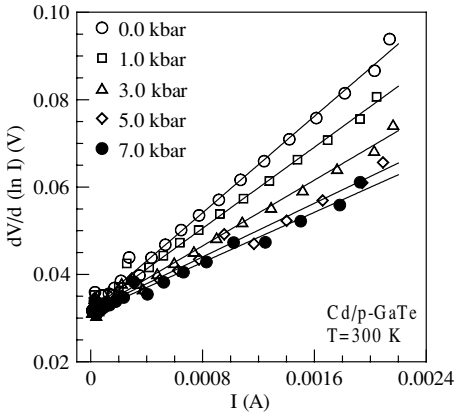

Figure 3. The experimental $dV/d(\ln I)$ versus I plots for the Cd/p-GaTe SBD in the pressure range of 0.0–7.0 kbar.

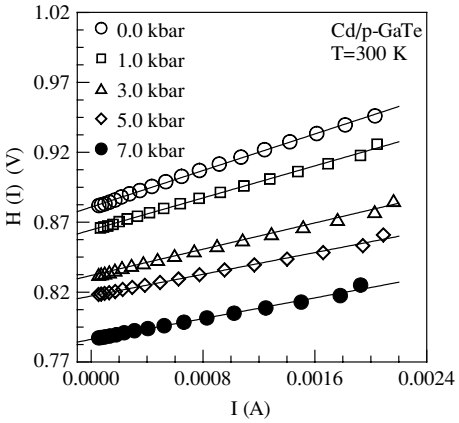

Figure 4. The experimental $H(I)$ versus I plots for the Cd/p-GaTe SBD in the pressure range of 0.0–7.0 kbar.

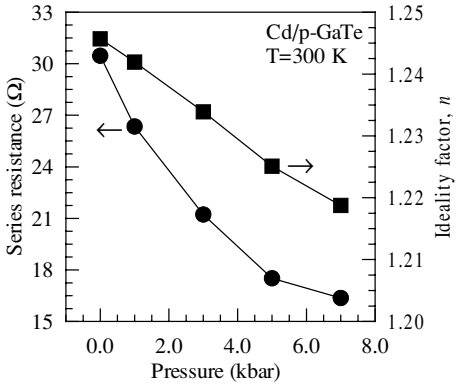

Figure 5. Pressure dependence of the series resistance (R_s) and the ideality factor (n) for the Cd/p-GaTe SBD.

Cd/p-GaTe SBD versus ambient pressure. As seen from this figure, there is a significant decrease in the series resistance with increasing pressure. The downward curvature in the forward bias I–V region for a sufficiently large applied voltage is due to the substrate resistance and to the continuum of the interface states. As seen in figure 1, the forward bias I–V curves deviate from linearity over approximately 0.30 V, but they become more and more straight with increasing pressure. The decrease in the series resistance is due to an improvement of the linearity of I–V curves at the high voltages with increasing pressure.

As can be seen in table 1, the values of the ideality factor n obtained from figures 1 and 3 differ slightly from each other, while their pressure dependence shows approximately a similar trend. Figure 5 also shows the plot of the averaged ideality factors n as a function of applied pressure with filled squares. As seen from this figure, there is a significant decrease in the n value with increasing pressure. The ideality factor n for an SBD is an empirical quantity and is defined as

$$n = \beta[\mathrm{d}V/\mathrm{d}\ln(I)], \tag{7}$$

where $\beta = q/kT$ for $V > 3/\beta$. As can be seen from equation (7) the slope directly affects the value of n. A decrease in the series resistance results in an increase in the diode current at the downward curvature region according to equation (2) and, hence, the ideality factor of the diode approaches unity with increasing pressure considering equation (7).

3.2. C–V measurements

In a C–V measurement carried out at sufficiently high frequency, the charge at the interface states cannot follow the ac signal. This will occur when the time constant is too long to permit the charge to move in and out of the states in response to an applied signal. Thus, for an SBD fabricated on a p-type semiconductor, the depletion layer capacitance can be expressed as [38]

$$\frac{1}{C^2} = \frac{2\,(V_{\mathrm{bi}} + V_{\mathrm{r}} - kT/q)}{q\varepsilon_{\mathrm{s}}\varepsilon_{\mathrm{o}}A^2N_{\mathrm{i}}}, \tag{8}$$

where, V_{bi} is the built-in voltage determined from the extrapolation of the C^{-2}–V plot to the voltage axis, V_{r} is the reverse voltage, A is the area of the diode, ε_{s} is the static dielectric constant equal to 7.3 for p-GaTe [19, 39], $\varepsilon_{\mathrm{o}} = 8.85 \times 10^{-14}$ F cm^{-1} and N_{i} is the concentration of the non-compensated ionized acceptors. N_{i} is related to the slope of C^{-2} versus V curve and can be obtained from the expression given below:

$$N_{\mathrm{i}} = \frac{2}{q\varepsilon_{\mathrm{s}}\varepsilon_{o}A^2}\left[\frac{1}{\mathrm{d}(C^{-2})/\mathrm{d}V}\right]. \tag{9}$$

The BH is obtained from

$$\Phi_{\mathrm{b}}(C - V) = V_{\mathrm{bi}} + V_{\mathrm{p}} + \frac{kT}{q} - \Delta\phi, \tag{10}$$

where V_{p}, referred to as the Fermi level potential, is the energy difference between the Fermi level and the top of the valence band, and given by $V_{\mathrm{p}} = kT/q[\ln(N_{\mathrm{v}}/N_{\mathrm{i}})]$. Thus, equation (10) can be rewritten by neglecting the image force barrier lowering, $\Delta\phi$, as

$$\Phi_{\mathrm{b}}(C - V) = V_{\mathrm{bi}} + \frac{kT}{q}\left[1 + \ln\frac{N_{\mathrm{v}}}{N_{\mathrm{i}}}\right], \tag{11}$$

where N_{v} ($= 1.17 \times 10^{19}$ cm^{-3}) is the effective density of states in the valence band for p-GaTe at 300 K. Figure 6 shows the reverse bias C^{-2}–V plots for the Cd/p-GaTe SBD as a function of pressure for a modulation frequency of 1.0 MHz. The capacitance of the Cd/p-GaTe SBD in the range of 0.0 to −1.0 V has increased with increasing pressure, as can be seen in figure 6. The linear behaviour of the curves can

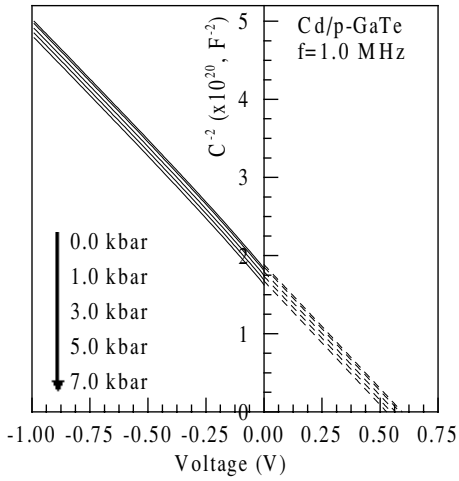

Figure 6. The reverse bias C^{-2}–V characteristics for the Cd/p-GaTe SBD as a function of hydrostatic pressure in the range of 0.0–7.0 kbar.

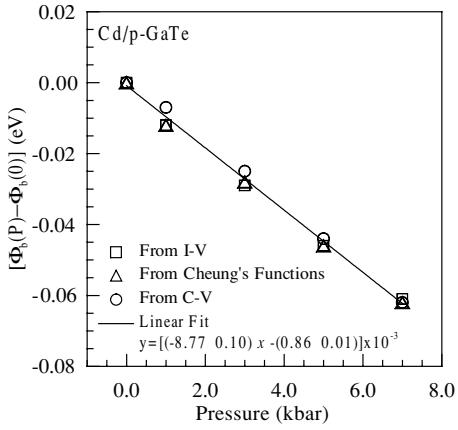

Figure 7. The change of SBHs for the Cd/p-GaTe SBD determined from I–V and C–V characteristics as a function of hydrostatic pressure. The solid line is a fitting curve to the averaged values of $(\Phi_b(P) - \Phi_b(0))$ obtained from I–V and C–V measurements.

be explained by the fact that the interface states and the inversion layer charge cannot follow the ac signal at 1.0 MHz and consequently do not contribute appreciably to the diode capacitance. V_{bi} and N_i values are obtained from the intercepts and the slopes of the extrapolated C^{-2}–V lines with the V_r axis, respectively. Then, the values of $\Phi_b(C-V)$ are calculated using equation (11). The N_i values obtained at different pressures, 2.41–2.43 $\times 10^{16}$ cm^{-3}, are in good agreement with the values determined from the Hall effect measurements [7, 17]. The values for the BH deduced from the C–V data are also shown in figure 2 as open triangles. The Φ_b and N_i values obtained from the C–V analysis as a function of pressure are also included in table 1. From the table, the $\Phi_b(C-V)$ values range from 0.780 eV at $P = 0.0$ kbar to 0.718 eV at $P =$ 7.0 kbar, while the N_i values of the device have remained approximately unchanged with increasing pressure.

In figure 2 and table 1, the $\Phi_b(C-V)$ values are seen to be higher than the $\Phi_b(I-V)$ values in the investigated pressure range. For the differences in BH values, some general reasons have been mentioned in the literature, such as surface contamination at the interface, deep impurity levels, an intervening insulating layer, quantum mechanical tunnelling, image-force lowering and edge leakage currents [35–37]. There have also been some reports showing that the discrepancy between BHs measured by different techniques might be associated with the instrumentation problems; namely, the way to determine true space-charge capacitance from C–V data or a large series resistance, which could affect the value determined from I–V data [40, 41]. Mönch [41] showed that both Schottky–Mott rule of BHs for metal–semiconductor contacts and Anderson's rule of the band-edge offsets for semiconductor heterostructures could not be applied to the layered crystals and some discrepancies shown in these materials may be ascribed to non-ideal interfaces. In our previous work, we have studied the temperature dependence of forward bias I–V characteristic of Cd/p-GaTe SBD using the TE theory with Gaussian distribution of the BHs around a mean value due to BH inhomogeneities prevailing in the MS interface [22]. Current transport at inhomogeneous SBDs is dominated by low-SBH regions leading to the determination of apparent SBHs by the I–V technique, which are lower than the mean value of the entire diode. Since the C–V technique yields an average SBH for the whole diode, the dependence of experimentally observed SBHs on the measurement technique is likely due to a distribution of SBHs.

On the other hand, we wish to consider the microstructures of the Cd/p–GaTe interface since their effects on SBHs are one of the fundamental issues in Schottky contacts. The effects of interface microstructures have been investigated and found to produce remarkable differences on SBHs. The different SBHs have been attributed to the difference of atomic arrangement at the interface [42]. The physical properties of GaTe are highly anisotropic since the bonding between the adjacent layers is considerably weaker than that of the intralayer. In GaTe, van der Waals forces contribute predominantly to the interlayer interaction while the bonding forces within the layers are primarily ionic-covalent type [1]. According to Mönch [41], metal/layered semiconductor SBHs show that the concept of interface-induced gap states (IFIGSs) consistently depicts the experimental data of layered semiconductors. Almeida *et al* [21] showed that metal-induced gap states (MIGSs), which tend to pin the Fermi level position (E_f) to maintain local charge neutrality, could be applied to the metal/GaTe interface. In general, these types of interface states affect the I–V behaviour of the diode because they may act as recombination centres or as intermediate states for trap-assisted tunnel currents. Therefore, this mechanism can increase the ideality factor and lower the BH values. C–V measurements are less prone to such defects because they are based on the ac technique, for this reason measure the average BH, regardless of the change in current. Therefore, these MIGSs can contribute to the difference observed for the two techniques.

The trend of the decreasing BH $\Phi_b(I-V)$ and $\Phi_b(C-V)$ with increasing pressure can be understood by the pressure dependence of the GaTe band gap. For this purpose, we show that the plot of BH changes as a function of pressure in figure 7 with different symbols for different techniques. There is a significant difference between the $\Phi_b(I-V)$ and $\Phi_b(C-V)$ values given in figure 2, while the BH changes $[\Phi_b(P) - \Phi_b(0)]$ found from those techniques are almost the

same and decrease linearly with increasing pressure as shown in figure 7. The variation in the BHs with pressure has been fitted with the equation

$$\Phi_b(P) = \Phi_0 + \alpha P, \tag{12}$$

where α (= $(-8.77 \pm 0.10) \times 10^{-3}$ eV kbar^{-1}) is the pressure coefficient of the BH. As mentioned above, for ideal Schottky diodes, MIGSs may be considered to be the physical mechanism determining the BHs [43]. According to the MIGS model of ideal metal–semiconductor contacts, the charge transferred between the metal and the semiconductor varies as a function of the position of the Fermi level relative to the intrinsic charge-neutrality level (CNL) of the MIGSs within the semiconductor band gap or as a function of the BH. No charge will be transferred across the interface when the Fermi level coincides with the intrinsic CNL of the MIGSs. In this case, the measured BH is called as the zero-charge-transfer barrier height (ZCTBH) and the pressure dependence of the BHs for the ideal Schottky contacts is determined by the pressure coefficient of the ZCTBHs [43]. Therefore, the pressure dependence of the ZCTBH for Schottky contacts on semiconductor substrates is determined by the respective variations of the width of the bulk band gap [43–45]. Werner and Güttler [46] and Werner [27] have concluded that the pressure and temperature coefficients of the SBHs depend on the chemical nature of the contact metal and the intrinsic effects of metal–semiconductor interface due to the different crystallography and interface topology, while lots of experimental results on the ideal Schottky contacts [44–49] have revealed that the Fermi level is pinned relative to the valance band or conduction band edge at the interface to explain both the external pressure and temperature dependence of the BH. Welber *et al* [45] also showed that the pressure coefficient of the BH for metal/GaAs Schottky contacts is the same as that of the fundamental gap of GaAs. The pressure dependence of the direct band gap of GaTe has been determined by Pellicer-Porres *et al* [50] up to 6.1 GPa and the pressure coefficient has been found to be -85.7 ± 0.4 meV GPa^{-1} (= -8.57 ± 0.04 meV kbar^{-1}) up to 2.9 GPa. In this study, the linear pressure coefficient of Cd/p-GaTe SBDs has been obtained as -8.77 ± 0.10 meV kbar^{-1} and this value is in close agreement with the value reported by Pellicer-Porres *et al* [50]. Thus, we may say that the pressure coefficient of the BH for the Cd/p-GaTe SBDs is almost the same as that found for the optical band gap of the GaTe in the investigated region.

In conclusion, the results obtained in the present study for Cd/p-GaTe SBDs may be explained by the MIGS model. We have concluded that the variation of the ZCTBH due to applied pressure should follow precisely the variation of the semiconductor band gap because the intrinsic CNL of the MIGSs or Fermi level has been accepted as a reference level which is pinned to the conduction-band minimum (CBM) as a function of the pressure.

References

[1] Lee P A (ed) 1976 *Optical and Electrical Properties of Layered Materials* (Dordrecht: Reidel)
[2] Lang O, Schlaf R, Pettenkofer C and Jaegermann W 1994 *J. Appl. Phys.* **75** 7805
[3] Teraguchi N, Kato F, Konagai M and Takahashi K 1991 *J. Electron. Mater* **20** 297
[4] Koma A 1999 *J. Cryst. Growth* **202** 236
[5] Klein A, Lehmann J, Pettenkofer C, Jaegermann W, Lux-Steiner M and Bucher E 1993 *Appl. Surf. Sci.* **70** 470
[6] Brebner J L, Fischer G and Mooser E 1962 *J. Phys. Chem. Solids* **23** 1417
[7] Güder H S 1999 *PhD Thesis* (in Turkish) Atatürk University Graduate School of Natural & Applied Science, Erzurum, Turkey (unpublished)
[8] Sánchez-Royo J F, Segura A and Muñoz V 1995 *Phys. Status Solidi* a **151** 257
[9] Wan J Z, Brebner J L and Leonelli R 1996 *Phys. Rev.* B **53** 15413
[10] Wan J Z, Brebner J L, Leonelli R and Graham J T 1992 *Phys. Rev.* B **46** 1468
[11] Wan J Z, Brebner J L, Leonelli R, Zhao G and Graham J T 1993 *Phys. Rev.* B **48** 5197
[12] Shigetomi S, Ikari T and Nishimura H 1998 *J. Lumin.* **78** 117
[13] Güder H S, Abay B, Efeoğlu H and Yoğurtçu Y K 2001 *J. Lumin.* **93** 243
[14] Pearson W B 1964 *Acta Crystallogr.* **17** 1
[15] Fischer G and Brebner J L 1967 *J. Phys. Chem. Solids* **23** 1363
[16] Augelli V, Manfredotti C, Murri R, Piccolo R, Rizzo A and Vasanelli L 1977 *Solid State Commun.* **21** 575
[17] Efeoglu H, Karaçalı T, Abay B and Yogurtçu Y K 2004 *Semicond. Sci. Technol.* **19** 523
[18] Shigetomi S, Ikari T and Nakashima H 1998 *Japan. J. Appl. Phys.* **37** 3282
[19] Manfredotti C, Murri R, Rizzo A, Vasanelli L and Micocci G 1975 *Phys. Status Solidi* a **29** 475
[20] Bose D N and Pal S 1997 *Phil. Mag.* B **75** 311
[21] Almeida J, Berger H and Margaritondo G 1998 *J. Appl. Phys.* **84** 1990
[22] Abay B, Çankaya G, Güder H S, Efeoğlu H and Yoğurtçu Y K 2003 *Semicond. Sci. Technol.* **18** 75
[23] Gulino D A, Faulkner L R and Drickamer H G 1983 *J. Appl. Phys.* **54** 2483
[24] Peanasky M J and Drickamer H G 1984 *J. Appl. Phys.* **56** 3471
[25] Çankaya G 1998 *MSc Thesis* (in Turkish) Atatürk University Graduate School of Natural & Applied Science, Erzurum, Turkey (unpublished)
[26] Çankaya G, Uçar N and Türüt A 2000 *Phys. Status Solidi* a **179** 469
[27] Werner J H 1989 *Appl. Phys. Lett.* **54** 1526
[28] Askerov D D, Agaev A M, Dzhaafarov T D and Ramazanzade M G 1984 *Phys. Status Solidi* a **83** 323
[29] Abdullaev G B, Akhundov M R and Akhundov G A 1966 *Phys. Status Solidi* **16** 209
[30] Micocci G, Melondini M and Tepore A 1991 *J. Appl. Phys.* **70** 6847
[31] Di Giulio M, Micocci G, Rizzo A and Tepore A 1983 *J. Appl. Phys.* **54** 5839
[32] Rhoderick E H and Williams R H 1988 *Metal–Semiconductor Contacts* (Oxford: Clarendon) pp 99–100
[33] Gouskov L, Gouskov A, Lemos V, May W and Sampaio H 1977 *Phys. Status Solidi* a **39** 65
[34] Cheung S K and Cheung N W 1986 *Appl. Phys. Lett.* **49** 85
[35] Sze S M 1981 *Physics of Semiconductor Devices* 2nd edn (New York: Wiley) pp 245–92
[36] Tung R T 1992 *Phys. Rev.* B **45** 13509
[37] Crowell C R 1977 *Solid-State Electron.* **20** 171
[38] Van der Ziel A 1968 *Solid State Physical Electronics* 2nd edn (Englewood Cliffs, NJ: Prentice-Hall)
[39] Camassel J, Merle P, Mathieu H and Gouskov A 1979 *Phys. Rev.* B **19** 1060
[40] Tung R T 2001 *Mater. Sci. Eng.* R **35** 1–138
[41] Mönch W 1998 *Appl. Phys. Lett.* **72** 1899
[42] Chung C K, Hwang J, Jaw T H and Wuu D S 2000 *Thin Solid Films* **373** 68
[43] Mönch W 2001 *Semiconductor Surfaces and Interfaces* 3rd edn (Berlin: Springer) pp 386–476

[44] Shan W, Li M F, Yu P Y, Hansen W L and Walukiewicz W 1988 *Appl. Phys. Lett.* **53** 974
[45] Welber B, Cardona M, Kim C K and Rodriguez S 1975 *Phys. Rev.* B **12** 5729
[46] Werner J H and Güttler H H 1993 *J. Appl. Phys.* **73** 1315
[47] Zhu S, Van Meirhaeghe R L, Detavernier C, Ru G P, Li B Z and Cardon F 1999 *Solid State Commun.* **112** 611
[48] Zhu S, Van Meirhaeghe R L, Detavernier C, Cardon F, Ru G P, Qu X P and Li B Z 2000 *Solid-State Electron.* **44** 663
[49] Phatak P, Newman N, Dreszer P and Weber E R 1995 *Phys. Rev.* B **51** 18003
[50] Pellicer-Porres J, Manjón F J, Segura A, Muñoz V, Power C and Gonzalez J 1999 *Phys. Rev.* B **60** 8871